ЖУРНАЛ СТРУКТУРНОЙ ХИМИИ

2017. Том 58, № 7 *Сентябрь – октябрь* *С. 1379 – 1387*

UDC 541.67

EXPERIMENTAL AND THEORETICAL STUDIES OF DIETHYL 2-(*TER*-BUTYLIMINO)-2,5-DIHYDRO-5-OXO-1-PHENYL-1H-PYRROLE-3,4-DICARBOXYLATE USING DFT CALCULATIONS

S. Yahyaei[1], E. Vessally[2], M. Hashemi[3]

[1]*Science and Research Branch, Islamic Azad University, Tehran, Iran*
[2]*Department of Chemistry, Payame Noor University, Tehran, Iran*
E-mail: vessally@yahoo.com
[3]*Department of Chemistry, Science and Research Branch, Islamic Azad University, Tehran, Iran*

Received December, 24, 2015 *Revised February, 11, 2016*

In this study, diethyl 2-(*ter*-butylimino)-2,5-dihydro-5-oxo-1-phenyl-1H-pyrrole-3,4-dicarboxylate compound **1** is synthesized and characterized by FT-IR, ^{1}H and ^{13}C NMR spectroscopy. The DFT calculations are carried out for compound **1** by B3LYP and PBE1PBE methods. The bond lengths, bond angles, dihedral angles, charge density on the atoms of **1** are calculated. A comparison of the DFT calculations indicate that the B3LYP method with the 6-311G++(*d*,*p*) basis set can give accurate results. The ^{13}C NMR and ^{1}H NMR chemical shifts of **1** are calculated and compared with the available experimental data on the molecules. The nuclear independent chemical shift (NICS) calculations are utilized for the pyrrole ring in compound **1**.

DOI: 10.26902/JSC20170710

K e y w o r d s: diethyl2-(*ter*-butylimino)-2,5-dihydro-5-oxo-1-phenyl-1H-pyrrole-3,4-dicarboxylate, DFT, FT-IR, GIAO, NMR chemical shifts, NICS calculation.

INTRODUCTION

Pyrrole derivatives are an important class of heterocycles. The nitrogen heterocycles are interesting compounds because they are applied in the synthesis of natural and non-natural products which exhibit useful biological activity [1]. Isocyanide-based multicomponent reactions have attracted much attention in modern chemistry because these reactions increase the efficiency by combining several operational steps without any isolation of intermediates or changes in the conditions [2—7]. Isocyanides are widely used in such reactions since they typically lead to the formation of cyclic and acyclic compounds. The nucleophilic character of the reactivity of isocyanides towards dimethyl acetylenedicarboxylate (DMAD) is well known [8—10]. The reaction of isocyanides with carbon—carbon triple bonds occurs in a one-pot reaction through a zwitterionic intermediate. As a continuation of our research [11], in this work, we report three-component reactions to synthesize diethyl 2-(*ter*-butylimino)-2,5-dihydro-5-oxo-1-phenyl-1H-pyrrole-3,4-dicarboxylate **1** (scheme 1) [12—20]. We also performed theoretical calculations of the geometrical parameters, vibrational analysis, and proton or carbon chemical shifts of **1** and compared them with the experimental data and the aromatic character of **1** is investigated in comparison with benzene.

EXPERIMENTAL

Synthesis and mechanism of the reaction. Starting materials and solvents were obtained from Merck (Germany) and Fluka (Switzerland) and were used without further purification. Three compo-

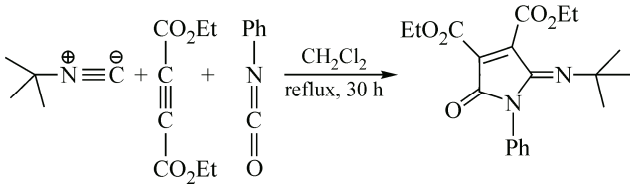

Scheme 1. Diethyl 2-(*ter*-butylimino)-2,5-dihydro-5-oxo-1-phenyl-1H-pyrrole-3,4-carboxylate

nents in this reaction are *t*-butyl isocyanides, diethylacetylenedicarboxylate, and phenyl isocyante. This one-pot synthesis proceeded spontaneously at 35 °C in CH_2C_{l2} and led to **1** (Scheme 1) [21]. The solution of *t*-butyl isocyanides (0.1 g, 1 mmol) in a dry CH_2Cl_2 (5 ml) solvent was slowly added dropwise to a mixture of phenyl isocyanate (0.1 g, 0.8 mmol) and DEAD (0.13 g, 0.8 mmol) in 25 ml of the CH_2Cl_2 solvent for 5 min. After the addition, the mixture was allowed to warm to room temperature and was refluxed at 35 °C for 30 h. Then, the solvent was removed under reduced pressure, and the yellow powder product was washed with a mixture of cold diethyl ether and *n*-hexane with a 1:3 ratio (2×3 ml). The liquid phase was filtered off and the precipitate was recrystallized in diethyl ether. The progress of the reactions was monitored by TLC and NMR techniques which indicated that there were no side products. The IR spectra were measured on Perkin—Elmer RXI and a FT—IR spectrometer. The ^1H and ^{13}C NMR spectra ($CDCl_3$) were recorded on a BrukerAvance spectrometer at 250.0 and 62.9 MHz, respectively. Elemental analyses were performed using a Perkin—Elmer 2400(II) CHN/O analyzer. The mass spectra were recorded on a FINNIGAN–MATT 8430 mass spectrometer operating at an ionization potential of 20 eV. The TLC plates were prepared from Merck silica gel powder. The synthetic route is shown in Scheme 1. A proposed reaction mechanism indicates that it is a three-component reaction between three compounds, which is presented in Scheme 2.

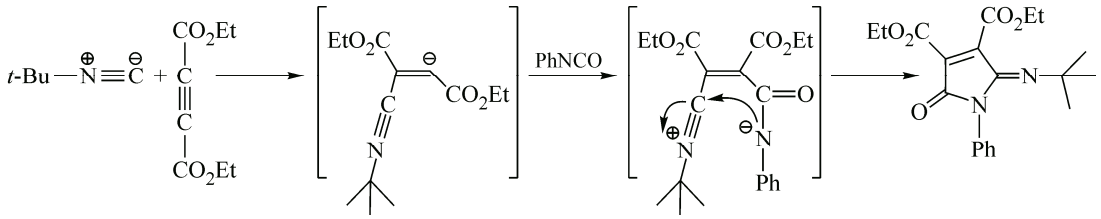

Scheme 2. A proposed mechanism for the synthesis of **1**

Diethyl 2-(*ter*-butylimino)-2,5-dihydro-5-oxo-1-phenyl-1H-pyrrole-3,4-dicarboxylate. Yellow crystals; yield 82 %, 0.31 g, m.p. 63—65 °C; IR (KBr) (ν max, cm^{-1}): 1744 and 1721 (2C=O of ester), 1668 (C=O). ^1H NMR (400.1 MHz, $CDCl_3$): δH 1.28 (9H, s, CMe_3), 1.38 and 1.40 (6H, 2t, $2CH_3$), 4.35 and 4.39 (4H, 2q, $2OCH_2$), 7.28—7.36 (5H, m, Ar—H). ^{13}C NMR (100.6 MHz, $CDCl_3$): δC 13.9 and 14.0 ($2CH_3$), 28.9 (CMe_3), 55.7 (N—CMe_3), 62.1 and 62.2 ($2OCH_2$), 123.1, 125.3, 127.7, 134.6, 137.4, 143.3 (C_{arom} and $C{=}C_{pyrrole\ ring}$), 147.4 (C=N), 148.0 (C=O), 159.5 and 159.6 (2C=O of ester). MS, *m*/*e* (%) = 373 (M++1, 14), 372 (M+, 5), 357 (80), 270 (62), 243 (30), 197 (75), 119 (28), 77 (24), 57 (40); Anal. Calcd for $C_{20}H_{24}N_2O_5$ (372.41): C 64.50, H 6.50, N 7.52 %. Found: C 64.43, H 6.58, N 7.44 %.

Computational details. In the present work, we carried out the theoretical investigation of **1**, using B3LYP and PBE1PBE methods with the 6-311++G(*d*,*p*) basis set. All calculations were carried out using the Gaussian 09 program [22]. The chemical shifts were calculated based on the GIAO approach and applied to the optimized molecule [23]. They were calculated by subtracting the appropriate isotopic part of the shielding tensor σ from that of TMS σ_{TMS}: $\delta = \sigma_{TMS} - \sigma$ (ppm). Furthermore, ^1H and ^{13}C chemical shifts were simulated using the GaussView software [24].

Table 1

Experimental (Exp.) *and calculated bond lengths* (Å) *and bond angles* (deg.) *for* **1** (*various methods and basis sets*)

Bond length	Exp.	B3LYP	PBE1PBE	Bond angles	Exp.	B3LYP	PBE1PBE
C1—C2	1.350	1.341	1.339	C1—C2—C3	108.16	108.650	108.512
C1—C6	1.477	1.489	1.483	C2—C3—N4	106.90	103.991	104.245
C1—C5	1.504	1.498	1.491	C2—C3—N9	130.65	137.216	137.965
C2—C3	1.490	1.514	1.505	C3—N4—C5	110.69	112.111	112.094
C3—N4	1.379	1.429	1.418	C3—C4—C16	126.06	124.535	124.603
C3—N9	1.271	1.256	1.254	C3—N9—C12	130.22	134.526	133.757
N4—C5	1.380	1.385	1.380	C1—C6—O44	113.18	111.486	111.726
N4—C16	1.434	1.428	1.418	N4—C5—C1	106.55	105.316	105.296
C5—O8	1.232	1.209	1.205	N4—C5—O8	124.75	126.899	126.854
C6—C10	1.203	1.211	1.208	C6—C1—C2	129.16	125.889	125.176
C6—O44	1.326	1.330	1.322	C6—O44—C45	115.57	117.327	116.520
N9—C12	1.487	1.466	1.455	O10—C6—O44	122.52	125.486	125.504
C12—C15	1.518	1.538	1.529	C15—C12—N9	108.16	113.996	114.236
O44—C45	1.470	1.455	1.441	O44—C45—C48	107.00	111.075	111.135
C45—C48	1.498	1.516	1.509				

RESULTS AND DISCUSSION

Geometrical structures and charges on the atoms. The global optimized configuration of **1** is shown in Scheme 3. The optimized structure was obtained by two calculation methods and compared with the experimental data; some of these data are listed in Tables 1—2. Correlations between the experimental and calculated bond lengths in the mentioned methods are shown in Fig. 1. As seen from Fig. 1, the B3LYP and PBE1PBE values ($R^2_{\text{bond length}} = 0.970$ and $R^2_{\text{bond length}} = 0.969$, respectively) are very close. The bond angles calculated at the B3LYP and PBE1PBE levels are in good agreement with the experimental values, those at the B3LYP level being slightly better [25—27]. The atomic polar tensor (APT) charges on the atoms of **1** were calculated at the B3LYP and PBE1PBE levels (Fig. 2) (Table 3). The highest positive charge located on the C_6 atom is +1.299 and +1.304 at the B3LYP and PBE1PBE levels, respectively. All charges on carbon atoms in the benzene ring are negative, except for C_{16}. All the oxygen and nitrogen atoms show negative charges. The highest negative charge is on

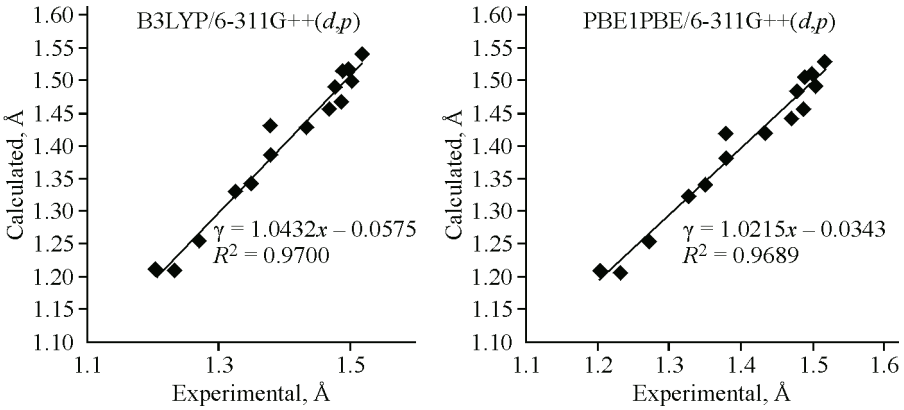

Fig. 1. Bond length correlations between the experimental and calculated data for **1**

Table 2

Experimental (EXP) *and calculated dihedral angles* (deg.) *for* **1** (*various methods and basis sets*)

Bond Dihedral	Exp.	B3LYP	PBE1PBE	Bond Dihedral	Exp.	B3LYP	PBE1PBE
C1—C2—C3—N4	–2.31	–3.84	–3.86	C5—N4—C3—C2	3.06	3.15	3.37
C3—C2—C1—C6	–178.62	–176.67	–176.69	O8—C5—N4—C3	–178.53	–179.38	–179.82
C3—N4—C5—O8	–178.53	–179.38	–179.82	C17—C16—N4—C5	72.90	60.73	53.23
C16—N4—C5—O8	1.28	2.36	2.00	C1—C5—N4—C16	–179.05	–179.66	–179.89
N4—C5—C1—C6	179.08	178.61	178.75	O10—C6—O44—C45	–1.89	–0.97	–0.17
N4—C5—C1—C2	1.08	–1.21	–0.90	C17—C16—N4—C3	–107.33	–117.31	–124.73
O8—C5—C1—C2	178.31	176.75	177.18	C1—C16—O44—C45	177.55	179.80	179.25

Table 3

Calculated charge density (e) *for* **1** (*various methods and basis sets*)

Charge density	B3LYP	PBE1PBE	Charge density	B3LYP	PBE1PBE	Charge density	B3LYP	PBE1PBE
C1	–0.306	–0.321	C7	1.225	1.234	C13	0.028	0.011
C2	–0.071	–0.063	O8	–0.790	–0.786	C16	0.370	0.385
C3	0.733	0.726	N9	–0.606	–0.589	O22	–0.856	–0.852
N4	–0.920	–0.946	O10	–0.767	–0.766	O44	–0.950	–0.943
C5	1.084	1.086	O11	–0.785	–0.786	C24	0.455	0.443
C6	1.299	1.304	C12	0.478	0.460			

the O_{44} and N_4 atoms (–0.950 — –0.920 and –0.946 — –0.943) at the B3LYP and PBE1PBE levels, respectively.

Vibrational assignments. The experimental FT—IR spectra of **1** are shown in Fig. 3. The studied molecule consists of 51 atoms. The number of normal vibrational modes of **1** was 147, including 111 in-plane (A') modes and 36 out-of-plane (A'') modes. Total of these vibrations were the sum of A' and A'' ($\Gamma_{vib} = 111A' + 36A''$).

C—H vibrations. In alkanes, alkenes, and aromatic structures the C—H stretching vibrations are in the ranges 2850—3000, 3010–3100, and 3000—3100 cm^{-1}, respectively [28, 29]. In FT-IR, the C—H stretching vibration was observed for alkane and the phenyl group at 2970 and 3056 cm^{-1},

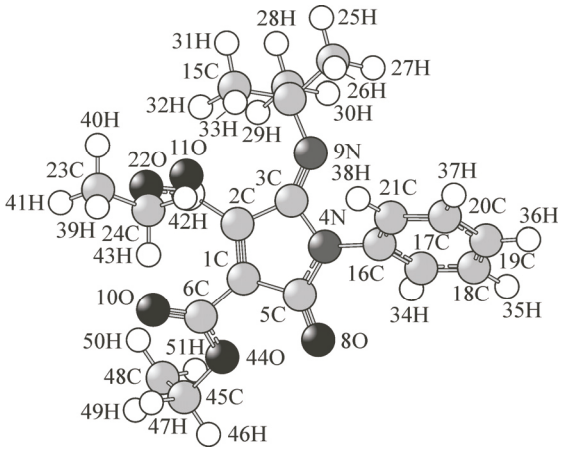

Scheme 3. Global optimized configuration of **1**

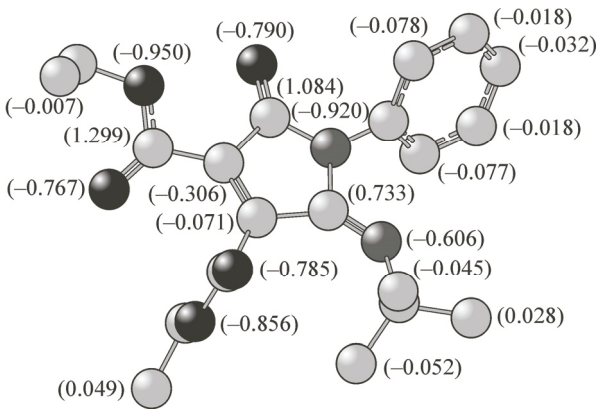

Fig. 2. Charges on the atoms of **1** calculated at the B3LYP/6-31++G(*d*,*p*) level

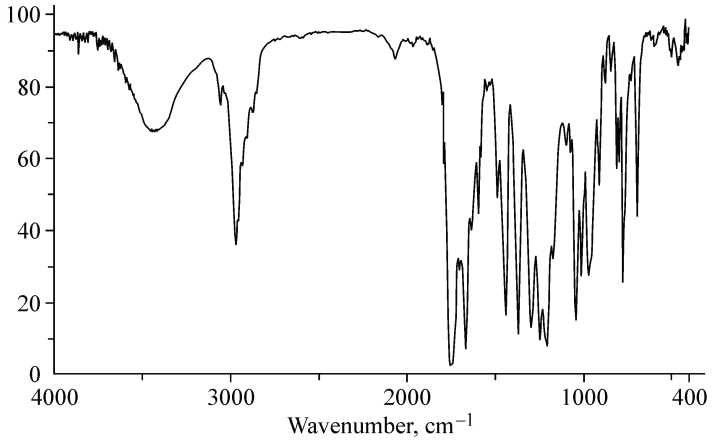

Fig. 3. Experimental IR spectra of **1**

respectively. The calculated C—H stretching vibrations appear at 2933 and 3053 cm^{-1} at the B3LYP/6-311++G(*d*,*p*) level, which was in good agreement with the experimental data. The calculated C—H stretching vibrations appear at 3032 and 3161 cm^{-1} at the PBE1PBE/6-311++G(*d*,*p*) level. As indicated by PED, the contributions of 89 and 88 % are at the B3LYP/6-311++G(*d*,*p*) level.

C=C vibrations. In alkenes and aromatic compounds the C=C stretching vibrations normally occur in the range 1620—1680 and 1400—1600 cm^{-1}, respectively [28, 29]. The C=C stretching vibrations are observed in the pyrrole ring at 1592 cm^{-1}. The calculated C=C stretching vibration appears at 1576 cm^{-1} at the B3LYP/6-311++G(*d*,*p*) level, which was in good agreement with the experimental data. The calculated C=C stretching vibration appears at 1646 cm^{-1} at the PBE1PBE/6-311++G(*d*,*p*) level. As indicated by PED, the contribution of 73 % is at the B3LYP level.

C=O vibrations. In esters and amides the C=O bond is observed in the ranges 1730—1750 and 1630—1690 cm^{-1}, respectively [28, 29]. In the title compound, the C=O bond is observed at 1744, 1721 for two esters and 1668 cm^{-1} for the amide functional group. The calculated C=O stretching vibration appears at 1722, 1718 for two esters and 1691 cm^{-1} for the amide functional group at the B3LYP/6-311++G(*d*,*p*) level, which was closer to the experimental data. The calculated C=O stretching vibration appears at 1812, 1808 for ester and 1777 cm^{-1} for amide at the PBE1PBE/6-311++G(*d*,*p*) level. As indicated by PED, the contributions of 78, 87, and 86 %, respectively, are at the B3LYP/6-311++G(*d*,*p*) level.

C=N vibrations. The C=N stretching absorption appears in the range 1640—1690 cm^{-1} [28, 29]. In this structure, the C=N bond is experimentally observed at 1635 cm^{-1}.The calculated C=N stretching vibration appears at 1656 cm^{-1} at the B3LYP/6-311++G(*d*,*p*) level, which was in good agreement with the experimental data. The calculated C=N stretching vibrations appear at 1740 cm^{-1} at the PBE1PBE/6-311++G(*d*,*p*) level. As indicated by PED, this mode (mode no. 28) involves the contribution of 75 % at the B3LYP/6-311++G(*d*,*p*) level. The relationship between the experimental and computed wavelength number of **1** obtained by B3LYP and PBE1PBE is presented in Fig. 4. The computed vibrational frequencies of **1** are in good agreement with the experimental values at the B3LYP level (R^2 = 0.9991) in contrast with the PBE1PBE level (R^2 = 0.9988) (Fig. 4). The comparison of two methods with the experimental vibrational frequencies for compound **1** is illustrated by Fig. 5. The graph shows that the frequencies calculated at the B3LYP level are closer to the experimental data.

Chemical shift analysis. Proton chemical shift analysis, ^{1}H NMR. The experimental ^{1}H NMR spectra of **1** are shown in Fig. 6. The ^{1}H chemical shifts (with respect to TMS) occur at 0.64—6.92 and 0.56—6.97 ppm at B3LYP and PBE1PBE levels, respectively, whereas the experimental shifts are observed at 1.28—7.31 ppm. The methyl protons ($H_{25—27}$, $H_{28—30}$, and $H_{31—33}$) experimentally resonate at 1.28 ppm as a singlet. These chemical shifts are theoretically predicted in the range of 0.67 and 0.64 ppm at the B3LYP and PBE1PBE levels of theory, respectively. The methyl protons of the ethyl groups ($H_{39—41}$ and $H_{49—51}$) experimentally resonate at 1.38 1.40 ppm as a triplet, these chemical shifts

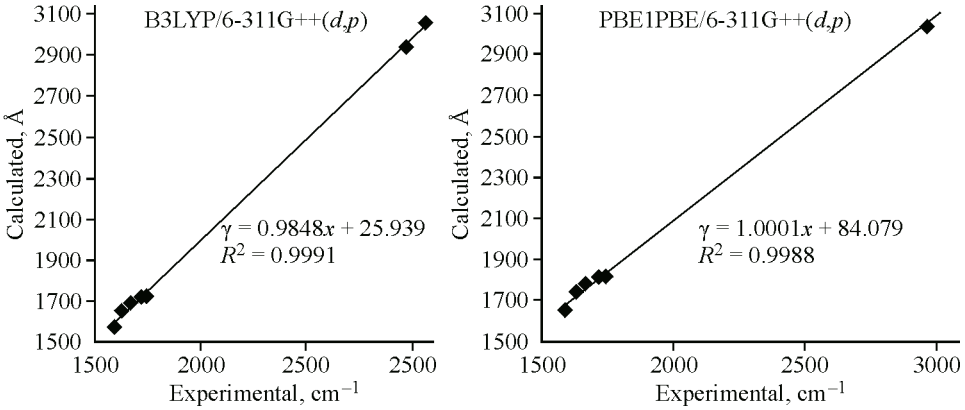

Fig. 4. Relationship between the experimental and computed frequencies of **1**

being theoretically predicted in the ranges 0.64—0.73 ppm and 0.56—0.65 at the B3LYP and PBE1PBE levels of theory, respectively. The signals at 4.37 ppm were assigned to methylene protons which experimentally resonate in the range of 3.96 and 3.81 ppm at the B3LYP and PBE1PBE levels of theory, respectively ($H_{42,43}$ and $H_{46,47}$). The multiplet at 7.31 ppm corresponds to the aromatic protons ($H_{34—38}$), which was calculated at 6.92 and 6.97 ppm at the B3LYP and PBE1PBE levels, respectively.

Carbon chemical shift analysis, ^{13}C NMR. The experimental ^{13}C NMR spectra of **1** are shown in Fig. 6, *b*. The ^{13}C chemical shift values (with respect to TMS) are observed in the range 10.40—165.79 and 9.81—163.34 ppm at the B3LYP and PBE1PBE levels, respectively, while the experimental results were located in the range 13.95—155.71 ppm. The chemical shift values of the ethyl group were experimentally observed at 13.95 and 62.15 ppm. The theoretical chemical shift values of these atoms were at 10.4 ($|\delta_{exp} - \delta_{B3LYP}| = 3.55$), 62.37 ($|\delta_{exp} - \delta_{B3LYP}| = -0.11$) at the B3LYP level, and 9.81 ($|\delta_{exp} - \delta_{PBE1PBE}| = 4.19$), 59.10 ($|\delta_{exp} - \delta_{PBE1PBE}| = 3.05$) at the PBE1PBE level, respectively. The chemical shifts of carbonyl groups were experimentally observed at 155.71 ppm. The theoretical chemical shifts of those atoms were calculated at 165.79 ($|\delta_{exp} - \delta_{B3LYP}| = -10.09$) at the B3LYP level, and 163.34 ($|\delta_{exp} - \delta_{PBE1PBE}| = -7.64$) at the PBE1PBE level, respectively. The relationship between the experimental and calculated ^{1}H and ^{13}C NMR chemical shifts for **1** is shown in Fig. 7. The B3LYP values of the chemical shift for ^{1}H and ^{13}C correlation ($R^2_{^1\text{H NMR}} = 0.9857$ and $R^2_{^{13}\text{C NMR}} = 0.9942$) were found to be in good agreement with the experimental values for ^{1}H NMR; in contrast, PBE1PBE values ($R^2_{^1\text{H NMR}} = 0.9855$ and $R^2_{^{13}\text{C NMR}} = 0.9949$) are better for ^{13}C NMR.

Aromatic character studies via NICS. The aromatic character is not a directly measurable or computable quantity. The magnetic criterion is measured through nucleus-independent chemical shift (NICS) ($0.5A^0$) calculation. It is based on a probe without basis functions (bq), which is placed at or above the geometrical center of a conjugated ring. The calculated isotropic NMR chemical shifts indicate the aromatic properties of the ring, either as an individual moiety in a polycyclic compound or as a molecule [30]. These studies usually require a comparison of non-aromatic compounds with a respective aromatic model compound. The aim of this research is to determine the aromatic character of

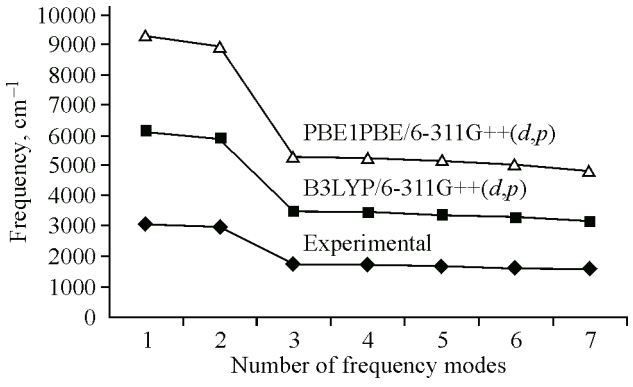

Fig. 5. Comparative experimental and computed frequencies (cm^{-1}) of two modes for **1**

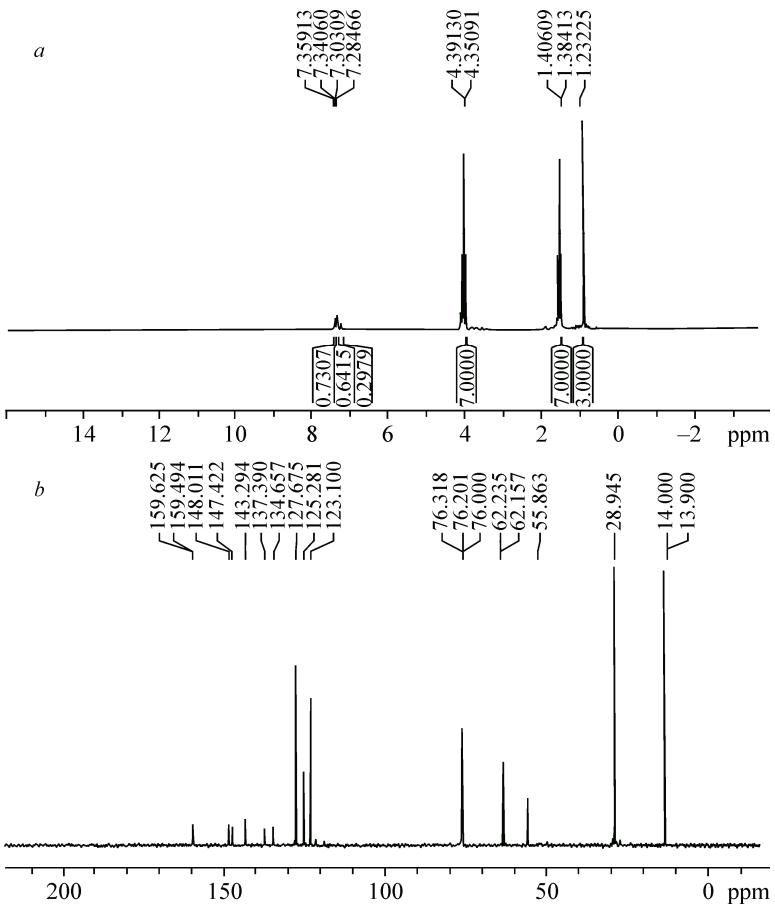

Fig. 6. Experimental ^{1}H NMR spectra (*a*) and ^{13}C NMR spectra (*b*)

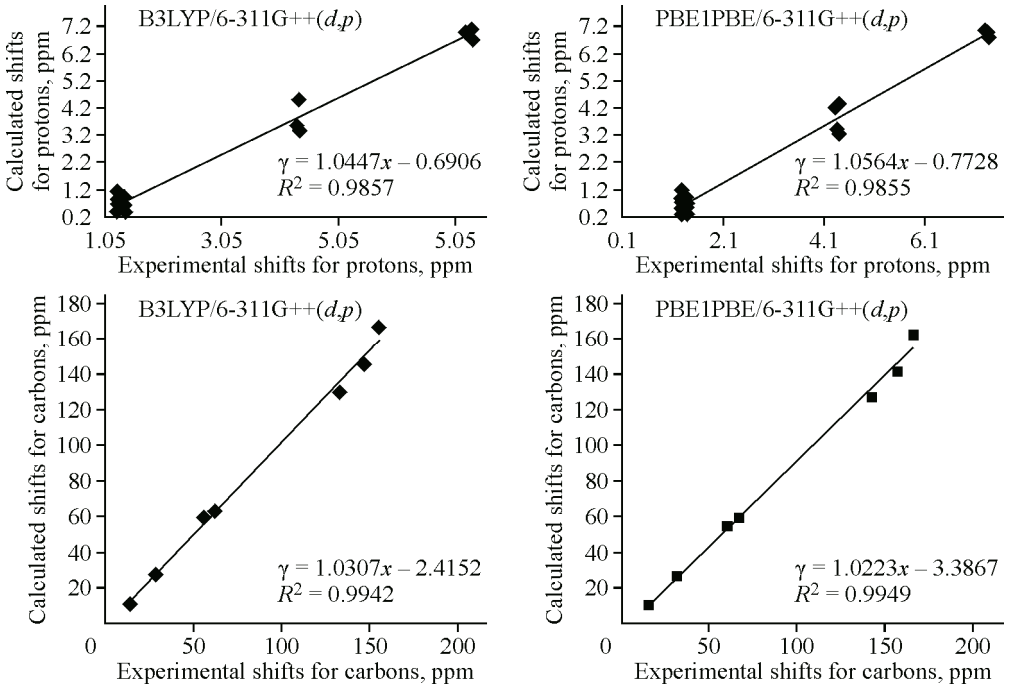

Fig. 7. Relationship between the experimental and calculated chemical shift for ^{1}H NMR of **1**

Table 4

NICS calculations for the aromatic determination of **1** (B3LYP *and* PBE1PBE *levels*)

Compound	Method	NICS(0)	NICS(0.5)	NICS(1)	NICS(1.5)	NICS(2)
Benzene	B3LYP	7.9720	9.6277	9.9804	7.3740	4.6220
Benzene	PBE1PBE	7.8104	9.7474	10.1356	7.4624	4.7165
1	B3LYP	0.9986	1.3729	1.3218	0.7523	0.4113
1	PBE1PBE	1.1155	1.4745	1.3744	0.7731	0.4328

1 in comparison with benzene. The aromatic character of **1** is investigated at B3LYP and PBE1PBE levels. The NICS calculation generally gives reliable results (Table 4).The results show the non-aromatic character of **1**.

CONCLUSIONS

The compound studied in this work, diethyl 2-(*ter*-butylimino)-2,5-dihydro-5-oxo-1-phenyl-1H-pyrrole-3,4-dicarboxylate **1**, has been obtained via the one-pot three-component (*t*-butyl isocyanides, diethyl acetylenedicarboxylate, and phenyl isocyanate) reaction. The structure of **1** was determined and characterized by the elemental analysis, FT-IR, ^{1}H and ^{13}C NMR. The comparison of B3LYP/6-311++G(*d*,*p*) and PBE1PBE/6-311++G(*d*,*p*) calculated and experimental values (bond lengths, bond angles, dihedral angles, vibrational wavenumbers, and chemical shifts for ^{1}H NMR of **1)** indicates that the B3LYP level is better than the PBE1PBE level of theory. Comparisons between the calculated ^{13}C NMR chemical shifts show that the PBE1PBE/6-311++G(*d*,*p*) level is found to be in good agreement with the experimental values. The result of the NICS calculation of **1** at the B3LYP and PBE1PBE levels indicate that it is a non-aromatic compound.

Acknowledgments. Science and Research Branch, Islamic Azad University is acknowledged. The authors gratefully acknowledge scientific comments on this research from Dr. A. Hosseinian.

REFERENCES

1. *Swinbourne J.F., Hunt H.J., Klinkert G.* // Adv. Heterocycl. Chem. – 1987. – **23**. – P. 103.
2. *Zhu J., Bienaym'e H.* (Eds) Multicomponent Reactions, Wiley—VCH, Weinheim, 2005.
3. *Orru R.V.A., Greef M.* // Synthesis. – 2003. – P. 1471 – 1499.
4. *Ramazani A., Shajari N., Mahyari A., Ahmadi Y.* // Mol. Divers. – 2011. – **15**. – P. 521 – 527.
5. *ZeinaliNasrabadi F., Ramazani A., Ahmadi Y.* // Mol. Divers. – 2011. – **15**. – P. 791 – 798.
6. *Ramazani A., ZeinaliNasrabadi F., MashhadiMalekZadeh A., Ahmadi Y.* // Monatsh. Chem. – 2011. – **142**. – P. 625 – 630.
7. *Ramazani A., Kazemizadeh A.R.* // Curr. Org. Chem. – 2011. – **15**. – P. 3986 – 4020.
8. *Ugi I., Werner B., Dömling A.* // Molecules. – 2003. – **8**. – P. 53 – 66.
9. *Astruc D., Lu F., Aranzaes J.R.* // Angew. Chem. Int. Ed. – 2005. – **44**. – P. 7852 – 7872.
10. *Beletskaya I.P., Cheprakov A.V.* // Chem. Rev. – 2000. – **100**. – P. 3009 – 3066.
11. *Asadi Z., Asnaashariisfahani M.B., Vessally E., Esrafili M.D.* // Spectrochim. Acta A. – 2015. – **140**. – P. 585 – 599.
12. *Lewis L.N.* // Chem. Rev. – 1993. – **93**. – P. 2693 – 2730.
13. *Banerjee S., Santra S.* // Tetrahedron Lett. – 2009. – **50**. – P. 2037 – 2040.
14. *Stefane B., Polanc S.* // Tetrahedron. – 2007. – **63**. – P. 10902 – 10913.
15. *Gotor V., Liz R., Testera A.* // Tetrahedron. – 2004. – **60**. – P. 607 – 618.
16. *Sibi M., Christensen J., Kim S., Eggen M., Stessman C., Oien L.* // Tetrahedron Lett. – 1995. – **36**. – P. 6209 – 6212.
17. *Ramazani A., Azizian A., Bandpey M., Noshiranzadeh N.* // Phosphorus, Sulfur, Silicon Relat. Elem. – 2006. – **181**. – P. 2731 – 2734.
18. *Yavari I., Ramazani A.* // Phosphorus, Sulfur, Silicon Relat. Elem. – 1997. – **130**. – P. 73 – 77.
19. *Ramazani A., Bodaghi A.* // Tetrahedron Lett. – 2000. – **41**. – P. 567 – 568.

20. *Ramazani A., Ahmadi Y., Rouhani M., Shajari N., Souldozi A.* // Heteroat. Chem. – 2011. – **21**. – P. 368 – 372.
21. *Khandan-Barani K., Maghsoodlou M., NourallahHazeri T., Habibi-Khorasani S.M., Sajadikhah S.S.* // ARKIVOC. – 2011. – **XI**. – P. 22 – 28.
22. *Frisch M.J. et al.* Gaussian 03, Revision 0.02, Gaussian, Inc., Wallingford CT, 2004.
23. *Ditchfield R.* // Mol. Phys. – 2008. – **27**. – P. 789.
24. *Dennington R.I.I., Keith T., Millam J.* GaussView Version 4.1.2, Semichem Inc., Shawnee Mission, KS, 2007.
25. *Bulatov E., Chulkova T., Haukka M.* // Acta Crystallogr. E. – 2014. – **70**. – P. o162.
26. *Anary-Abbasinejad M., Mirhosseini M., Tabatabaee M.* // Acta Crystallogr. E. Struct. – 2010. – **17**. – P. o1101.
27. *Akkurt M., Mohamed S.K., Elremaily M.A., Santoyo-Gonzalez F., Albayati M.R.* // Acta Crystallogr. E. – 2013. – **69**. – P. o1761-2.
28. *Rastogi V.K., Palafox M.A., Tanwar R.P., Mittal L.* // Spectrochim. Acta A. – 2002. – **58**. – P. 1987 – 2004.
29. *Silverstein R.M., Basseler G.C., Morill T.C.* / Spectrometric Identification of Organic Compounds, 4th ed. – New York: John Wiley and Sons., QD272, S6 S55, 1981.
30. *Vessally E., Nikoorazm M., Ramazani A.* // Chines J. Inorg. Chem. – 2008. – **124**, N 4. – P. 631 – 635.